Severing of F-Actin by the Amino-Terminal Half of Gelsolin Suggests Internal Cooperativity in Gelsolin

Lynn A. Selden,* Henry J. Kinosian,# Jay Newman,§ Bryan Lincoln,§ Charles Hurwitz,* Lewis C. Gershman,*#¶ and James E. Estes*#

*Research Service and ¶Medical Service, Stratton Veterans Affairs Medical Center, and #Department of Physiology and Cell Biology and ¶Department of Medicine, Albany Medical College, Albany, New York 12208, and §Department of Physics, Union College, Schenectady, New York 12308 USA

ABSTRACT Gelsolin is a Ca^{2+}-regulated actin-binding protein that can sever, cap, and nucleate growth from the pointed ends of actin filaments. In this study we have measured the binding of the amino-terminal half of gelsolin, G1–3, to pyrene-labeled F-actin as a function of Ca^{2+} concentration. The rate of binding is shown to be dependent on micromolar concentrations of Ca^{2+}. Independent experiments demonstrate that conformational changes in G1–3 are induced by micromolar concentrations of Ca^{2+}. Titrations of pyrene-F-actin with G1–3 and gelsolin show that the quenching of pyrene fluorescence is identical in extent and stoichiometry for both G1–3 and gelsolin. In contrast, severing of F-actin by G1–3 is found to be much less efficient than is severing by gelsolin. In experiments in which F-actin severing is quantitatively measured, the filament number is found to be proportional to the 1.35 power of the G1–3 concentration. This deviation from linearity may be explained by cooperativity; the binding of two G1–3 molecules in close proximity may lead to cooperative severing of the polymer, thus increasing the severing efficiency. This model is supported by experiments that show that the efficiency of G1–3 severing of F-actin increases with increasing G1–3:F-actin ratios. Extrapolating from these results, we conclude that G4–6, the carboxyl-terminal half of gelsolin, has an active role in the severing of F-actin by intact gelsolin. Whereas F-actin severing by G1–3 is enhanced by cooperative binding of two separate G1–3 molecules, cooperativity is inherent to intact gelsolin because the cooperative partners are covalently linked.

INTRODUCTION

Gelsolin is an actin-binding protein that can sever and cap actin filaments and nucleate actin filament assembly in a Ca^{2+}-dependent manner (Yin and Stossel, 1979; Yin et al., 1981; Kurth et al., 1983). The efficient severing of F-actin by gelsolin in the high-Ca^{2+} environment of serum aids in the clearance of actin from the bloodstream after tissue damage (Haddad et al., 1990; Vasconcellos and Lind, 1993). The function of gelsolin within cells is less obvious because the relatively low intracellular Ca^{2+} concentrations are below those required for efficient activation of gelsolin function (Lamb et al., 1993). Several studies have shown that gelsolin is down-regulated in a variety of cancer cell lines (Vandekerckhove et al., 1990; Asch et al., 1996), and a recent study shows that gelsolin can be proteolyzed into its amino-terminal and carboxyl-terminal fragments by caspase, a protein induced during cell apoptosis (Kothakota et al., 1997). The caspase-generated amino-terminal fragment was shown to sever actin polymers at the low Ca^{2+} concentrations found within the cell (Kothakota et al., 1997).

Gelsolin contains six highly homologous repeat segments, called G1 to G6, respectively (Kwiatkowski et al., 1989), and the crystal structure of intact gelsolin (Burtnick et al., 1997) as well as that of G1 complexed with actin have been determined (McLaughlin et al., 1993). Ca^{2+} regulation of gelsolin is thought to be a cooperative process in which the Ca^{2+} binding to the carboxyl-terminal domain causes a conformational change that opens the molecule to allow actin binding to occur (Kwiatkowski et al., 1989; Hellweg et al., 1993). Until recently, the Ca^{2+} concentration required for this conformational change has been thought to be in the micromolar range (Kilhoffer and Gerard, 1985; Allen and Janmey, 1994) However, Pope et al. (1997) have now shown that this conformational change occurs at ~50 nM Ca^{2+}. As gelsolin function appears to be regulated at Ca^{2+} concentrations much higher than 50 nM (Lamb et al., 1993; Allen and Janmey, 1994), it may be that functional regulation of gelsolin is modulated by Ca^{2+} binding to other gelsolin domains after the molecule is opened.

The exact mechanism of F-actin severing by gelsolin is not clear. There is general agreement that G2 contains an F-actin binding site that positions G1 for strong binding to the polymer, causing a disruption between the actin-actin contacts that results in severing (McLaughlin et al., 1993). This idea has been supported by the observation that the amino-terminal half of gelsolin (G1–3) severs F-actin, whereas the carboxyl-terminal segment (G4–6) does not (Bryan and Hwo, 1986). Because severing by G1–3 was found to occur in the absence of Ca^{2+}, it is generally assumed that Ca^{2+} regulation of gelsolin resides in the carboxyl-terminal half of the molecule (Chaponnier et al., 1986; Way et al., 1989). However, it is well known that the G1 segment of gelsolin binds one or two Ca^{2+} molecules

Received for publication 26 May 1998 and in final form 27 August 1998.

Address reprint requests to Dr. James E. Estes, Research Service (151), Stratton VA Medical Center, 113 Holland Avenue, Albany, NY 12208. Tel.: 518-462-3311; Fax: 518-462-0626; E-mail: estes.james_e@albany.va.gov.

0006-3495/98/12/3092/09 $2.00

upon binding to actin, depending on the ionic conditions (Weeds et al., 1995).

In a previous publication we demonstrated that the fluorescence intensity of pyrene-F-actin is quenched upon binding of gelsolin to actin. At high Ca^{2+} concentrations, the binding reaction is diffusion controlled whereas the severing reaction is a first-order reaction with a relatively slow rate constant of 0.3 s^{-1} (Kinosian et al., 1996). In this report we confirm that the G1–3 binds with high affinity to F-actin both in the presence and in the absence of Ca^{2+}. However, the rate of binding as well as the conformation of G1–3 are modulated by Ca^{2+}. We further demonstrate that the binding of G1–3 does not necessarily result in severing; the severing process appears to be cooperative, requiring the binding of two G1–3 molecules in close proximity. This is in contrast to the case for intact gelsolin in which the binding of one gelsolin molecule results in one F-actin severing event. The cooperative severing of F-actin by G1–3 suggests that the binding of G4–6 may be a necessary step for efficient severing of F-actin by intact gelsolin.

MATERIALS AND METHODS

Actin from rabbit skeletal muscle was purified by published procedures and column purified by size exclusion chromatography (Kinosian et al., 1993). Actin was labeled in the polymer form with fivefold molar excess of *N*-pyrenyl-iodoacetamide, collected by centrifugation, depolymerized by dialysis, and clarified for 1 h at 200,000 × *g* before use (Kinosian et al., 1993). Monomeric pyrene actin, typically 15–30 μM, was converted to Mg-actin by a 5-min incubation with 100 μM $MgCl_2$ and 100 μM EGTA before being polymerized by addition of 0.1 M KCl. Phalloidin was added to the actin for stopped-flow experiments to minimize depolymerization, but not for light-scattering experiments, which were done at 10 μM actin. In these experiments the small change in critical concentration (~0.5 μM) in the presence of gelsolin had a negligible effect on the F-actin diffusion coefficient.

G1–3 was expressed in *E. coli* kindly provided by Dr. Helen Yin and contains the amino-terminal 406 amino acids of gelsolin (Yu et al., 1991). The protein was collected in inclusion bodies, dissolved in 8 M urea and allowed to refold by dialyzing out the urea. The preparation was then collected as the flow-through of a DEAE-Sepharose FF column with 25 mM Tris, 1 mM EGTA, pH 8, as eluant. The DEAE flow-through was applied in the same buffer to a CM-Sepharose FF column and eluted with a 0–0.5 M NaCl gradient. The protein was >99% pure by electrophoresis and, based on comparison to gelsolin, was fully functional in F-actin binding (c.f. Fig. 1) and capping (data not shown).

Stopped-flow measurements

All experiments included buffers containing 0.1 M KCl and either 10 mM MOPS/Tris, pH 7.0, or 10 mM Tris/HCl, pH 8. Care was taken to control the temperature as the pK_a of Tris is temperature dependent. Experiments were accomplished with 1:1 mixing from a stopped-flow device with a dead time of 20 ms (Hi-Tech SFA-11) or 1 ms (SLM-Aminco Milliflow). These devices were connected (respectively) to an SLM-Aminco SPF 500 or an Aminco Bowman Series 2 spectrofluorimeter for fluorescence measurements. Excitation was at 365 nm with 4–5 nm bandpass, and emission was at 386 nm with a bandpass of 4–10 nm.

For the stopped-flow experiments one syringe contained pyrene-F-actin diluted to 100 nM with buffer containing 0.1 M KCl and 4 μM phalloidin to minimize depolymerization, and the second syringe contained the same buffer with twice the desired concentrations of G1–3, $CaCl_2$, EGTA, and $MgCl_2$. Free Ca^{2+} concentrations were calculated using a computer program (Perrin and Sayce, 1967). Fura-2-FF (Texas Fluorescence Labs, Austin, TX) was used to determine Ca^{2+} in our buffers, as an indicator in titrations of EGTA, and to confirm the affinity constants used to calculate free Ca^{2+}.

The stopped-flow experiment at each condition was repeated five to eight times, and the data from the repeats were averaged. The data curves are biphasic and are well fit by the sum of two exponentials:

$$F = F_0 + F_1(e^{-k1t}) + F_2(e^{-k2t})$$

For the experiments in this manuscript, k_{obs} refers to *k1* in the first exponential. The second exponential is >10-fold slower than the first, allowing relatively clean separation of the two processes.

Dynamic light scattering

Actin at 30 μM was filtered directly into cuvettes, converted to Mg-actin by addition of 0.1 mM $MgCl_2$ and 0.1 mM EGTA (final concentrations), and diluted to 10 μM, with 5 mM HEPES, 0.1 M KCl, 2 mM $MgCl_2$, 0.2 mM ATP, 0.2 mM $CaCl_2$, pH 7. Sample volumes ranged from 0.4 to 1 ml. The polymerization process was monitored by dynamic light scattering (DLS). G1–3 or gelsolin was then added, the sample was mixed very gently, and the diffusion coefficient was monitored by DLS. DLS data were obtained at room temperature using a 514.5-nm laser beam and a scattering angle of 90°. The diffusion coefficient (*D*) was determined by cumulant analysis.

Filament severing assays

Solutions of F-actin (10% pyrene labeled), typically 25–200 nM in 5 mM HEPES, 0.2 mM ATP, 2 mM $MgCl_2$, 0.1 M KCl, 5 μM phalloidin, pH 7.0, were added in 1-ml aliquots to cuvettes and allowed to incubate for several hours to allow filament annealing to occur (Kinosian et al., 1993). The sample was placed in the sample compartment and the fluorescence intensity recorded. Then $CaCl_2$ was added to 100 μM and either G1–3 or gelsolin was added to the desired concentration. The sample was mixed gently and the fluorescence intensity continuously monitored. After 100 s (all observed samples had reached a steady fluorescence plateau within 100 s), 1 ml of 3 μM Mg-actin monomer solution was added through the top of the fluorimeter sample cover directly into the cuvette in the sample holder. The fluorescence intensity increase was then recorded as a function of time. In addition to the initial rate, the fluorescence intensity of each sample was measured after complete polymerization had occurred. The fluorescence increase per micromolar F-actin was determined from known amounts of polymer. The number of filament ends was calculated based on a pointed-end elongation rate constant of 1 μM^{-1} s^{-1} (Kinosian et al., 1996), subtracting the number of ends determined in controls at each F-actin concentration (without severing protein). This assay assumes that G1–3 remains bound and caps the barbed filament ends after severing. We confirmed this in separate experiments (not shown) in which as little as 0.5 nM G1–3 was shown to prevent polymerization of 0.5 μM Mg-actin in the presence and absence of Ca^{2+}. Given the rapid binding of G1–3 to F-actin in the presence of Ca^{2+} (see Fig. 2) and the large ratio of F-actin side-binding sites to filament end-binding sites, we conclude that very little G1–3 binds directly to filament ends. The presence of phalloidin ensures that there is essentially no monomer present, eliminating the possibility of competition between actin monomer and polymer for G1–3 binding. Thus, we conclude that G1–3 caps are formed by G1–3 remaining bound to a filament end after a severing event.

RESULTS

Binding of G1–3 to Mg-F-actin polymer

Fig. 1 shows the titration of pyrene-Mg-F-actin (stabilized by phalloidin) with G1–3 or gelsolin. The data are plotted as

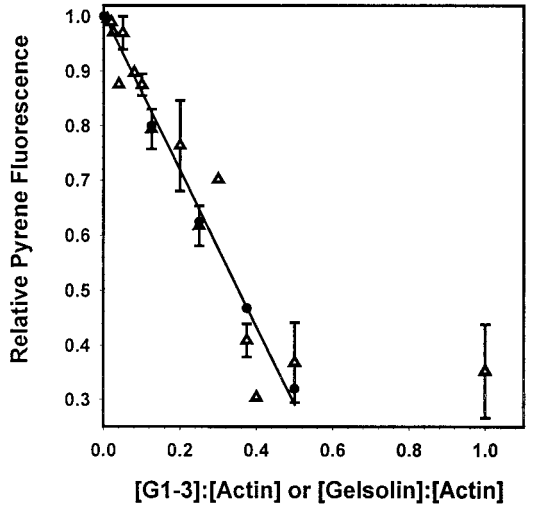

FIGURE 1 Titration of F-actin with G1–3 and gelsolin. Polymer actin was 10% pyrene labeled, at concentrations ranging from 25 nM to 200 nM in 0.1 M KCl, 2 mM $MgCl_2$, 5 mM HEPES, 0.2 mM ATP, 0.1 mM $CaCl_2$, 5 μM phalloidin, pH 7.0. G1–3 △ or gelsolin ● was added to the sample and the fluorescence recorded. Fluorescence intensity values were normalized to 1 by dividing by the fluorescence intensity measured in the absence of G1–3 or gelsolin. Error bars are standard deviations of different experiments at the same G1–3:actin ratios. The line is a fit to the G1–3 data up to G1–3:actin = 0.5. The line fit to the gelsolin data is statistically indistinguishable.

a ratio of G1–3:F-actin, allowing comparison of different actin concentrations on the same plot. There is a decrease in fluorescence intensity with increasing G1–3 or gelsolin concentration. Saturation of the quenching reaction occurs at a 1:2 molar ratio of either protein to actin. Identical results were obtained at F-actin concentrations varying from 25 to 200 nM, demonstrating the high affinity of G1–3 for actin.

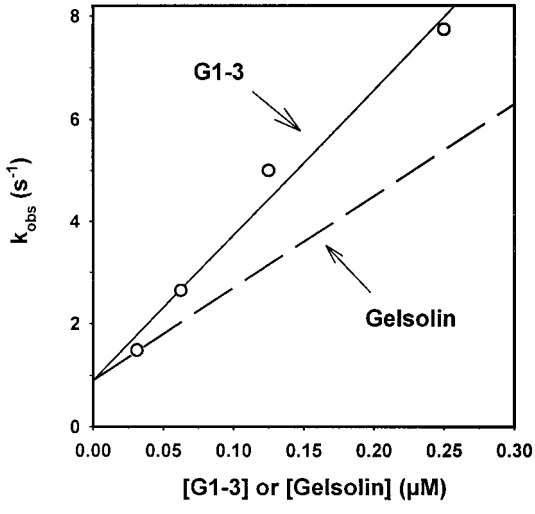

FIGURE 2 Rate constant for G1–3 association with Mg-F-actin. Data are from stopped-flow experiments conducted as described in Materials and Methods. The Ca^{2+} concentration was 100 μM. The solid line through the data yields a second-order rate constant for G1–3-Mg-F-actin association of 2.8×10^7 M^{-1} s^{-1}. The dashed line, drawn for comparison, represents a second-order rate constant of 1.8×10^7 M^{-1} s^{-1}, the rate that we previously determined for gelsolin (Kinosian et al., 1996).

At Ca^{2+} concentrations above 5 μM, the kinetics of the fluorescence intensity decrease shown in Fig. 1 are similar to those observed for gelsolin at 500 μM Ca^{2+} (Kinosian et al., 1996). Thus, the decrease in pyrene fluorescence intensity appears to reflect quenching caused by binding of G1–3 to actin, and this signal can be used to investigate the effects of pH and Ca^{2+} on the interaction between G1–3 and F-actin. Fig. 2 shows a plot of k_{obs} versus G1–3 concentration at high Ca^{2+} concentrations. The linear fit yields a second-order rate constant of 2.8×10^7 M^{-1} s^{-1} for the G1–3-F-actin interaction. For reference, the dashed line indicates a rate constant of 1.8×10^7 M^{-1} s^{-1} that we previously determined for intact gelsolin at 500 μM Ca^{2+} (Kinosian et al., 1996).

Effect of Ca^{2+} on the binding of G1–3 to Mg-F-actin

The observed rate constant for G1–3 binding to F-actin at varying Ca^{2+} concentrations was determined from stopped-flow measurements. In these experiments, 1 μM G1–3 in the presence of various Ca^{2+} concentrations was reacted with 100 nM phalloidin-stabilized Mg-F-actin. Fig. 3 *A* shows typical time course data for an experiment performed at 1, 12.5, and 80 nM free Ca^{2+}, whereas Fig. 3 *B* shows the results of experiments at pH 7.0 and 8.0 over a large range of Ca^{2+} concentrations. Complete binding occurs at pH 7.0 in the presence of 1 nM Ca^{2+}, but the rate of binding is much slower than at higher Ca^{2+} concentrations. At pH 8.0, higher Ca^{2+} concentrations are required to obtain binding rates comparable to those obtained at pH 7.0. In contrast to the pH 7.0 results, G1–3 binding to F-actin at pH 8.0 is extremely slow and incomplete below 3 μM Ca^{2+}. G1–3 binding was also affected to a small extent by the presence of Mg^{2+}. At low concentrations of Ca^{2+}, where the G1–3-F-actin binding rate was slow, addition of $MgCl_2$ in the millimolar range increased the rate of binding in a concentration-dependent manner (data not shown), but not to the levels attainable with micromolar concentrations of Ca^{2+}. Overall, the most striking finding from this kinetic study is that there is a dramatic increase in the rate of G1–3 binding to F-actin as the Ca^{2+} concentration is increased to micromolar levels at pH 7 and pH 8.

To address the question of whether the enhanced rate of G1–3 interaction with F-actin by increased Ca^{2+} concentrations arises from Ca^{2+}-induced conformational changes in the G1–3 molecule, we investigated the effects of Ca^{2+} on the intrinsic fluorescence of G1–3. Fig. 4 shows the fluorescence emission of G1–3 and gelsolin in the presence and absence of Ca^{2+} and the resultant difference spectra. Ca^{2+} binding apparently induces conformational changes within G1–3 that increase the tryptophan fluorescence. The effect of Ca^{2+} on the tryptophan fluorescence of intact gelsolin is the opposite, apparently due to solvent quench as

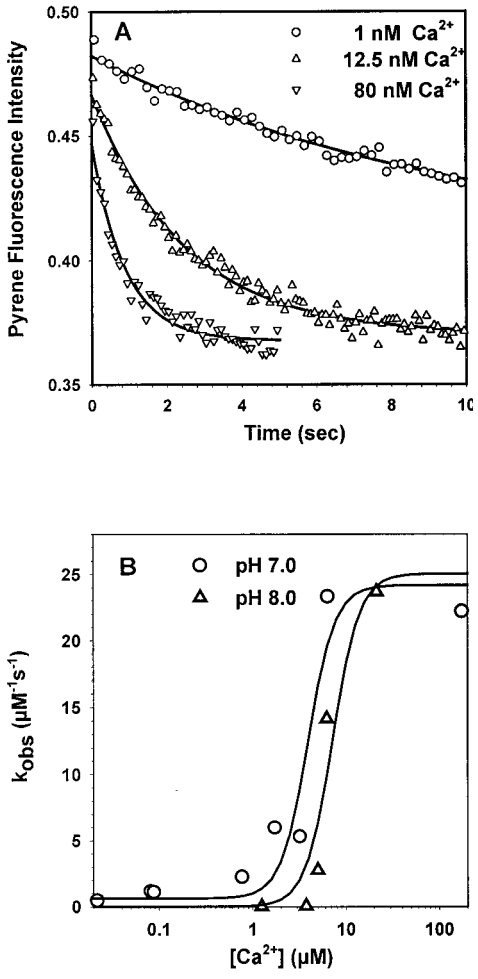

FIGURE 3 Kinetics of G1–3 binding to F-actin are Ca^{2+} dependent. (*A*) Fluorescence intensity data collected in typical stopped-flow experiment. Syringe 1 contained 100 nM F-actin in 0.1 M KCl, 10 mM MOPS, 0.2 mM ATP, 10 μM $CaCl_2$, 4 μM phalloidin, pH 7.0. Syringe 2 contained 1 μM G1–3 in 10 mM MOPS, pH 7.0, and either 5.0, 0.4, or 0.075 mM EGTA to adjust the free Ca^{2+} to 1, 12.5, or 80 nM, respectively. Data are averages of five repeats at each condition. The endpoints at 200 s were identical for all three conditions (not shown). (*B*) Individual experiments were performed essentially as shown in *A* but with the Ca^{2+} adjusted over a higher free concentration range using EGTA. Contaminant Ca^{2+} in the buffers was determined using Quin 2. At pH 8, 10 mM Tris buffer was substituted for MOPS. Values for k_{obs} were calculated from the double exponential fits to the data as described in Materials and Methods.

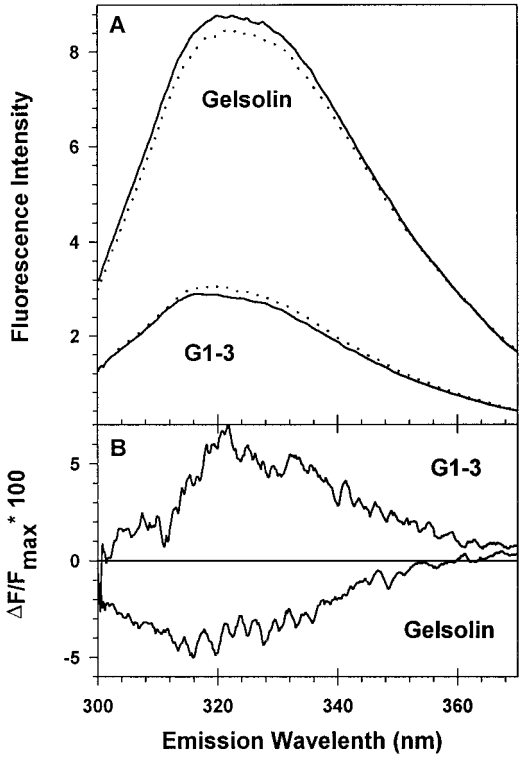

FIGURE 4 The effect of Ca^{2+} on tryptophan fluorescence from G1–3 and gelsolin. G1–3 or gelsolin, 0.5 μM, in 5 mM MOPS, 0.1 M KCl, 0.2 mM ATP, 0.1 mM EGTA, pH 7.0, in the absence (——) or in the presence (· · ·) of 0.3 mM $CaCl_2$. (*A*) Fluorescence was excited at 295 nm, and a 2-nm bandpass was used for both excitation and emission. Data were collected in the ratio mode, Raman scatter was subtracted, and the instrument correction was applied. (*B*) The difference spectra with and without Ca^{2+} for G1–3 and gelsolin. The difference spectra are expressed as the percentage of the peak fluorescence to adjust for the roughly threefold difference between the fluorescence intensities at equal concentrations.

the gelsolin molecule opens up after binding of Ca^{2+} within the carboxyl-terminal half. These results, combined with the results of Fig. 3, suggest that Ca^{2+} binding triggers conformational changes within G1–3 that enhance the interaction between G1–3 and F-actin. Similar changes may occur in intact gelsolin, but may be masked by quenching of tryptophan in other domains.

Severing of F-actin by G1–3

The data presented thus far demonstrate that G1–3 binds to phalloidin-stabilized Mg-F-actin in a Ca^{2+}-dependent manner, but the actual severing activity of G1–3 has not yet been addressed. We previously demonstrated that severing of F actin by intact gelsolin occurs by rapid formation of an F-actin-gelsolin complex followed by a relatively slow (0.3 s^{-1}) severing step (Kinosian et al., 1996). In initial studies of F-actin severing by G1–3 we used DLS measurements. This technique is noninvasive and provides a reasonable physical measurement of relative average filament lengths. Fig. 5 shows the results of a DLS experiment conducted at 10 μM F-actin (without phalloidin) with varying concentrations of G1–3 and gelsolin. It is apparent from these measurements that F-actin severing by G1–3 is not as efficient as severing by gelsolin. Filament severing by gelsolin in the range of gelsolin:actin ratios of 0.005–0.02 yields a nearly linear plot whereas G1–3 appears to sever F-actin with a much lower efficiency until the G1–3:actin ratio reached 0.2.

Although the DLS measurements show that G1–3 is less efficient than gelsolin at severing F-actin, these measurements also suggest that F-actin severing by G1–3 becomes more efficient as the G1–3:actin ratio is increased. However, DLS measurements alone do not provide accurate estimates of filament number over an extended G1–3 con-

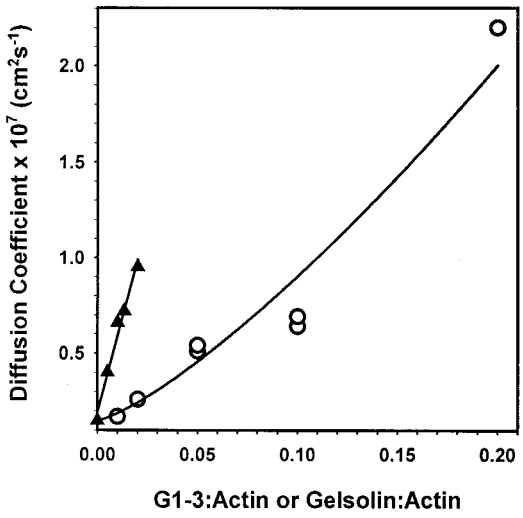

FIGURE 5 DLS measurements of F-actin severing by gelsolin and G1–3. Indicated concentrations of gelsolin (▲) or G1–3 (○) were achieved by addition of 37 μl of gelsolin or G1–3 to 10 μM Mg-F-actin in 5 mM HEPES, 0.2 mM ATP, 0.1M KCl, 2 mM $MgCl_2$, 100 μM $CaCl_2$, pH 7.0. The diffusion coefficient was determined as described in Materials and Methods.

centration range. Therefore, we developed a filament severing assay for more precise determinations of filament number. Fig. 6 shows data from such experiments with 200 nM F-actin. The inset shows the severing data at low G1–3 and gelsolin concentrations. To evaluate the curvature, a power curve was fit to the data between G1–3:actin ratios of 0 and 0.3. In this range, the increase in filament number m is described by: $m = 0.1 \times [\text{G1–3}]^{1.35}$. Above G1–3:actin ratios of 0.3, the number of ends appeared to plateau so that even at a 1:1 G1–3:actin ratio, full severing did not occur.

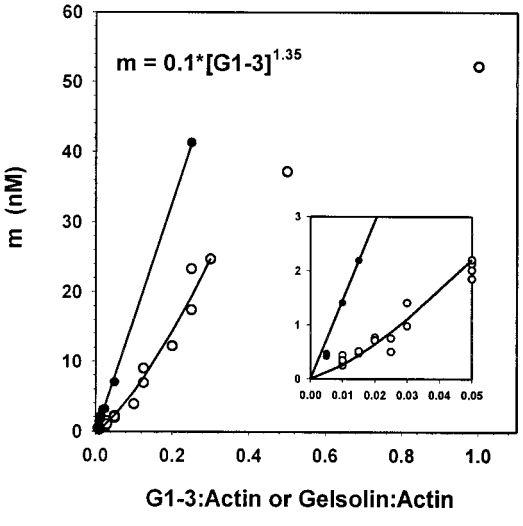

FIGURE 6 Filament severing at increasing gelsolin:actin and G1–3:actin ratios. The number of filament ends m produced at different gelsolin or G1–3 concentrations and 200 nM Mg-F-actin was determined as described in Materials and Methods. The gelsolin data (●) were fit by a linear least-squares line with a slope of 0.95, and the G1–3 data, at G1–3:actin ratios less than 0.3 were fit with the equation $m = 0.1 \times [\text{G1–3}]^{1.35}$. The inset provides an expanded view of the lower concentration range of gelsolin and G1–3.

One way to explain the data in Figs. 5 and 6 is to postulate that severing by G1–3 is a cooperative process requiring more than one G1–3 molecule. If this is the case, one might expect the efficiency of severing to increase as the G1–3:actin ratio increases, as it appears to do in the 0.01–0.03 G1–3:actin range shown in Fig. 6. Therefore, we studied the efficiency of G1–3 severing at F-actin concentrations from 25 to 200 nM. At each F-actin concentration, the G1–3 concentration was varied in regular increments to yield a range of G1–3:actin ratios, and the number of filament ends generated at each condition was measured. As shown in Fig. 7, the efficiency, defined as the number of ends generated divided by the G1–3 concentration, increases as the G1–3:actin ratio increases. The maximal efficiency occurs above a G1–3:actin ratio of 0.5. The lowest efficiencies measured were in the 0.1–0.2 range at low G1–3:actin ratios. If binding is random at very low G1–3:actin ratios, the probability that two G1–3 molecules will bind to the filament in close proximity is low. The severing that occurs at these low ratios could be due to weakening of the filament caused by G1–3 binding with subsequent filament severing during the mixing phase of the assay. Alternatively, binding of one G1–3 could cause a change in the structure that then increases the probability for binding a second G1–3. Either scenario would produce cooperative severing by G1–3 consistent with the data.

DISCUSSION

A model for cooperative severing of F-actin

The most important finding reported here is that severing of F-actin by G1–3 is a cooperative process. That F-actin

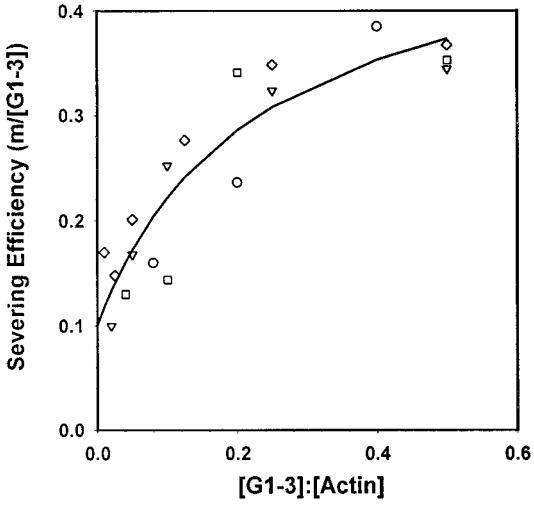

FIGURE 7 Increasing severing efficiency with increasing G1–3:actin ratio. The number of filament ends, m, was determined as described in Materials and Methods. The F-actin concentration was 25 nM (○), 50 nM (□), 100 nM (△), and 200 nM (◇). The efficiency of severing was calculated as the filament number m divided by the G1–3 concentration.

severing efficiency is increased by binding of more than one G1–3 molecule in close proximity has implications for the mechanism by which gelsolin severs actin filaments. The amino-terminal half of gelsolin is considered effective in severing actin filaments (Chaponnier et al., 1986; Way et al., 1989, Kwiatkowski et al., 1989). Our data extend this view to one in which the F-actin severing efficiency is greatly enhanced by the cooperative binding of another G1–3 in close proximity. In intact gelsolin, the carboxyl-terminal half, G4–6, may serve a similar purpose. Until now G4–6 has been thought to contribute primarily to capping actin filaments (Way et al., 1989). However, G4–6 is known to compete with G1–3 for binding to actin, and there is some evidence that G2–6 has weak F-actin severing activity (Way et al., 1989).

F-actin severing by cooperative binding of gelsolin's G1–3 and G4–6 regions to actin could offer an explanation for the findings in our recent report on the kinetics of F-actin severing by gelsolin (Kinosian et al., 1996). In that work we found that irreversible binding of gelsolin occurred quickly (diffusion controlled), whereas severing of the polymer was much slower (0.3 s^{-1}). The data presented here in Fig. 1 show that the extent of pyrene-F-actin fluorescence quenching and the stoichiometry of the binding reaction are identical for G1–3 and gelsolin although the extent of severing is different (Fig. 6). This provides strong evidence that the fluorescence quenching signals the binding of the G1–3 portion of whole gelsolin, but not the severing. We propose that the severing reaction is inevitable or completed when G4–6 binds to a site on the opposite strand of the polymer. The combined binding provides enough energy for disruption of the actin-actin bonds of both strands, and efficient severing occurs. The relatively long time required for the severing process would then be explained by rearrangements that occur within the gelsolin molecule to accommodate binding of G4–6 to the filament. Fig. 8, *A* and *B*, shows our interpretation of cooperative severing by G1–3 and intact gelsolin. As shown in Fig. 8 *A*, binding of one molecule of G1–3 to F-actin results in a low probability for severing of the filament. From extrapolation of Fig. 7 data, the efficiency appears to be ~10% (0.1 cuts per G1–3). Binding of another G1–3 in close proximity, however, increases the probability for severing to 1, yielding an efficiency of 50% (one cut per two G1–3) At low ratios of gelsolin, shown in Fig. 8 *B*, an inherent cooperativity due to the presence of G4–6 exists resulting in efficient severing.

As shown in Fig. 8 *C*, an interesting possibility arises at high gelsolin:actin ratios. The binding of the amino-terminal of regions of two different gelsolin molecules could act cooperatively in a manner similar to that observed for G1–3. In this case, the G4–6 regions are inhibited from binding. McGough et al. (1998) concluded from electron microscopic reconstructions of filaments decorated at high G2–6:actin ratio, that G4–6 is not bound to the actin filament. The data shown in Fig. 8 *D* are consistent with the models depicted in Fig. 8, *B* and *C*. Efficient F-actin severing by gelsolin is predicted by the solid line. At low gelsolin:actin ratios, one filament is generated per gelsolin, but at high gelsolin:actin ratios, fewer filaments are formed than predicted. As the model in Fig. 8 *C* suggests, filaments smaller than four to five subunits cannot be generated by gelsolin severing. Experiments performed without phalloidin could lead to different results as the gelsolin-actin complexes may rapidly rearrange by depolymerization to yield gelsolin-actin dimer complexes.

Effect of phalloidin on the measurements

The majority of the experiments make use of phalloidin stabilization of pyrene-labeled F-actin to prevent depolymerization from occurring. This simplifies the analysis because in the absence of depolymerization the decrease in pyrene fluorescence is attributable only to the binding reaction. We believe that the results are not greatly affected by the presence of phalloidin. The dynamic light-scattering experiments were conducted without addition of phalloidin. The diffusion coefficient measurements from these experiments show a cooperative behavior similar to the direct measurements of elongation rates. The line drawn in Fig. 5 was generated by the same equation, $D \propto [G1–3]^{1.3}$, used to fit the data in Fig. 6. In contrast, the gelsolin data in both figures are fit by a straight line.

Measurements of severing at low Ca^{2+} concentrations indicate that the rate, but not the extent, of severing of F-actin by gelsolin is slowed approximately twofold in the presence of phalloidin (data not shown). At high Ca^{2+} concentrations, little difference was observed (Kinosian et al, 1998). Similar experiments with G1–3 (not shown) revealed no differences with and without phalloidin at the physiologic conditions used in our experiments. Overall, the effect of phalloidin on the severing of F-actin appears to be relatively small.

Effects of Ca^{2+}

Work from several laboratories has shown that regulation of the gelsolin molecule by Ca^{2+} is more complex than originally thought. Certain functions of gelsolin appear to be activated by Ca^{2+} in the 1 μM range whereas others have been reported to be activated at levels of from 10 to 100 μM (Lamb et al., 1993; Allen and Janmey, 1994; Ditsch and Wegner, 1995). The recent work by Pope et al. (1997) provides key insights into the multiple functions conferred by Ca^{2+} binding to gelsolin. Their studies demonstrate that a major conformational change that opens the gelsolin molecule occurs at submicromolar concentrations of Ca^{2+}. They hypothesize that regulation of gelsolin function occurs by additional Ca^{2+} binding at other, secondary sites within the gelsolin molecule. Our data support this hypothesis.

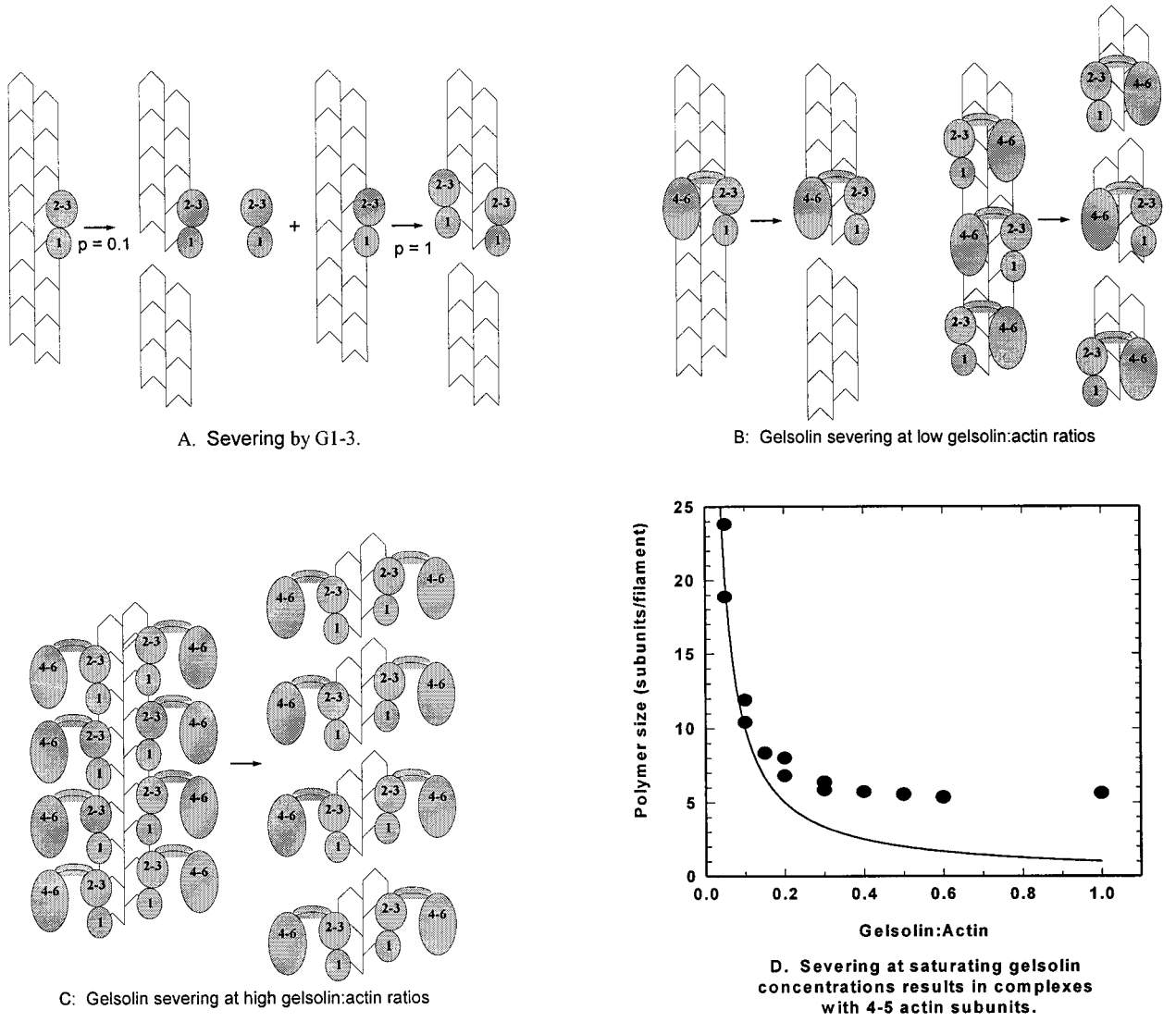

FIGURE 8 (*A*) Severing efficiency of G1–3. The diagram illustrates how two molecules of G1–3 bind cooperatively to F-actin to sever the filament. The model is based on the work of McGough et al. (1998), which shows that G2–3 is bound between two longitudinally adjacent monomers in the actin filament and G1 binds to actin subdomains 1 and 3 on the lower monomer. From Fig. 7, it appears that the probability that a single G1–3 molecule will sever an actin filament is ~0.1 (efficiency = 10%). The probability that an actin filament with one G1–3 bound will be severed after another G1–3 binds to the opposite strand is very high, resulting in a 50% severing efficiency (one severing event per two molecules of G1–3) (*B*) Gelsolin severing of actin filaments at low (≤1:5) gelsolin:actin ratios. Cooperative G4–6 binding on the opposite strand results in efficient severing. (*C*) As the gelsolin:actin ratio increases beyond 1:5, further rapid binding of G1–3 to the filament prevents binding of G4–6, resulting in a reduced severing efficiency. (*D*) Samples of 100 nM Mg-F-actin stabilized with 2 μM phalloidin were severed by a 60-s incubation with varying concentrations of gelsolin in polymerizing buffer containing 500 μM $CaCl_2$. The rate of elongation on addition of 1 μM pyrene-labeled Mg-ATP-actin was used to calculate the filament number concentration *m*, as described in Materials and Methods. The data are expressed as filament length by dividing *m* by the F-actin concentration.

As binding of G1–3 or gelsolin to F-actin is essentially irreversible, the slower rate of binding at lower Ca^{2+} concentrations (Fig. 3, *A* and *B*) does not alter the amount of protein bound at equilibrium, only the time to reach equilibrium. With gelsolin, the irreversible process can be stopped by allowing the molecule to close by reducing Ca^{2+} to very low concentrations, thereby reducing the rate of binding to zero. On the other hand, the G1–3 segment of the gelsolin molecule apparently cannot be completely closed at low Ca^{2+} concentrations, and thus, the binding and severing by G1–3 cannot be completely stopped.

The relevance of the effects of Ca^{2+} binding to G1–3 to alterations of gelsolin function is not clear. From Fig. 3 *B*, the rate of G1–3 binding to actin is seen to increase dramatically at ~5 μM Ca^{2+}. This Ca^{2+} concentration is similar to that at which Pope et al. (1997) noted dissociation of G1 from G2–6. On the other hand, intact gelsolin binding to actin begins to be regulated at micromolar concentrations of Ca^{2+} and continues to increase throughout a range extending to near millimolar concentrations (Allen and Janmey, 1994). Whether Ca^{2+} binding by the G4–6 or Ca^{2+}-dependent cooperative behavior is involved remains to be elucidated.

Relationship to previous studies of G1–3

The importance of the amino-terminal half of gelsolin in F-actin severing is well established (Way et al., 1989; Kwiatkowski et al., 1989). Ca^{2+} regulation of the severing reaction within the amino-terminal region of gelsolin was reported in truncates of gelsolin as small as the amino-terminal 160 amino acids and as large as the amino-terminal 237 amino acids, but no Ca^{2+} regulation of F-actin severing by G1–3, which contains the amino-terminal 407 amino acids, was noted (Kwiatkowski et al., 1989). Pope et al. (1997) report 1.4 Ca^{2+} sites per G1–3 with a dissociation constant of ~0.2 μM. Our finding that the rate of G1–3 binding to actin increases with Ca^{2+} concentration is in concurrence with a Ca^{2+} binding site located within G1–3.

The increase in G1–3 tryptophan fluorescence intensity with increasing Ca^{2+} is in contrast to a decrease in tryptophan fluorescence intensity noted for gelsolin under similar conditions (Fig. 4). Pope et al. (1997) noted that the Stokes radius of gelsolin increases with Ca^{2+} concentration while the Stokes radius of G1–3 decreases with increased Ca^{2+} concentrations. Our tryptophan fluorescence measurements of G1–3 probably reflect this, since a more compact protein structure is likely to have a tryptophan environment shielded from the quenching effects of the solvent.

Literature reports comparing the severing efficiency of G1–3 with gelsolin vary from 87% (Way et al., 1989) to 50% (Bryan and Hwo, 1986), but the increase in efficiency of F-actin severing with increasing G1–3:actin ratio has not been previously reported. It is difficult to make direct comparisons between our work and that of others due to different assay conditions. We have some evidence suggesting that binding of G1–3 to the polymer weakens the filament, resulting in a shear-sensitive polymer (Lincoln et al., 1998). In the experiments presented here, we were very careful to minimize shear during sample manipulation.

Physiologic implications

Within the last decade it has become apparent that there are a large number of proteins that share homology with the segments of gelsolin. One result of cooperative F-actin severing through the binding of a severing protein to two sites in close proximity is that the amount of severing increases nonlinearly with the concentration of severing protein. In the case of G1–3, severing increases in proportion to the 1.35 power of the G1–3 concentration. This implies that it is not necessary for G1–3 to bind to a single neighboring subunit on F-actin. Rather, binding to one of two or three nearby subunits on the opposite F-actin strand may be enough to cause severing. Other proteins, typically termed weak severing proteins (i.e., actin depolymerizing factor) may require binding at two or more specific sites to provide enough binding energy to sever the filament. Such behavior would exhibit greater cooperativity and would amplify the effect of the concentration of severing protein on the amount of filament severing. Thus, in a cell, increased expression of a weak severing protein could result in a disproportionately large amount of filament severing.

Summary

In this study we have measured the binding and severing of F-actin filaments by the G1–3 fragment of gelsolin. We have demonstrated cooperativity of G1–3 severing of F-actin filaments suggesting that severing occurs by the binding of two molecules in close proximity. This is in contrast to the very efficient F-actin severing characteristic of intact gelsolin. These observations lead to a model for F-actin severing by gelsolin that includes G4–6 as an active participant in the F-actin severing process. We have also noted that the binding of G1–3 to F-actin is a Ca^{2+}-regulated process. This observation supports the recent suggestions by Pope et al. (1997) that the functional characteristics of gelsolin are differentially regulated by Ca^{2+} binding at different sites within different parts of gelsolin. The complex interrelationships between these Ca^{2+}-binding sites and the organization of the gelsolin segments remain a challenge for future studies.

We thank Dr. P.A. San Biagio and Dr. D. Bulone, visiting professors from CNR-IAIF and Physics Departments, University of Palermo, Palermo, Italy, for performing preliminary dynamic light scattering measurements. We also thank the reviewers for their insightful comments.

This work was supported by the Department of Veterans Affairs grant 0398–002 (L.C. Gershman), National Institutes of Health grant GM 32007 (J.E. Estes), and National Science Foundation grant MCB 9316025 (J. Newman).

REFERENCES

Allen, P. G., and P. A. Janmey. 1994. Gelsolin displaces phalloidin from actin filaments. A new fluorescence method shows that both Ca^{2+} and Mg^{2+} affect the rate at which gelsolin severs F-actin. *J. Biol. Chem.* 269:32916–32923.

Asch, H. L., K. Head, Y. Dong, F. Natoli, J. S. Winston, J. L. Connolly, and B. B. Asch. 1996. Widespread loss of gelsolin in breast cancers of humans, mice, and rats. *Cancer Res.* 56:4841–4845.

Bryan, J., and S. Hwo. 1986. Definition of an N-terminal actin-binding domain and a C-terminal Ca^{2+} regulatory domain in human brevin. *J. Cell Biol.* 102:1439–1446.

Burtnick, L. D., E. K. Koepf, J. Grimes, E. Y. Jones, D. I. Stuart, P. J. McGlaughlin, and R. C. Robinson. 1997. The crystal structure of plasma gelsolin: implications for actin severing, capping and nucleation. *Cell.* 90:661–670.

Chaponnier, C., P. A. Janmey, and H. L. Yin. 1986. The actin filament severing domain of plasma gelsolin. *J Cell Biol.* 103:1473–1481.

Ditsch, A., and A. Wegner. 1995. Two low affinity Ca^{2+} binding sites of gelsolin that regulate association with actin. *Eur. J. Biochem.* 229: 512–516.

Haddad, J. G., K. D. Harper, M. Guoth, G. G. Pietra, S. W. Sanger. 1990. Angiopathic consequences of saturating the plasma scavenger system for actin. *Proc. Natl. Acad. Sci. U.S.A.* 87:1381–1385.

Hellweg, T., H. Hinssen, and W. Elmer. 1993. The Ca^{2+}-induced conformational change of gelsolin is located in the carboxyl-terminal half of the molecule. *Biophys. J.* 65:799–805.

Kilhoffer, M. C., and D. Gerard. 1985. Fluorescence study of brevin, the 92,000 actin-capping protein isolated from serum: effect of Ca^{2+} on protein conformation. *Biochemistry*. 24:5653–5660.

Kinosian, H. J., J. Newman, B. Lincoln, L. A. Selden, L. C. Gershman, and J. E. Estes. 1998. Ca^{2+} regulation of gelsolin activity: binding and severing of F-actin. *Biophys. J.* 75:3101–3109.

Kinosian H. J., L. A. Selden, J. E. Estes, and L. C. Gershman. 1993. Actin filament annealing in the presence of ATP and phalloidin. *Biochemistry*. 32:12353–12357.

Kinosian, H. J., L. A. Selden, J. E. Estes, and L. C. Gershman. 1996. Kinetics of gelsolin interaction with phalloidin-stabilized F-actin: rate constants for binding and severing. *Biochemistry*. 35:16550–16556.

Kothakota, S., T. Azuma, C. Reinhard, A. Klippel, J. Tang, K. Chu, T. J. McGarry, M. W. Kirschner, K. Koths, D. J. Kwiatkowski, and L. T. Williams. 1997. Caspase-3-generated fragment of gelsolin: effector of morphological change in apoptosis. *Science.* 278:294–298.

Kurth, M. C., L.-L. Wang, J. Dingus, and J. Bryan. 1983. Purification and characterization of a gelsolin-actin complex from human platelets. *J. Biol. Chem.* 258:10895–10903.

Kwiatkowski, D. J., P. A. Janmey, and H. L. Yin. 1989. Identification of critical functional and regulatory domains in gelsolin. *J. Cell Biol*. 108:1717–1726.

Lamb, J. A., P. G. Allen, B. Y. Tuan, and P. A. Janmey. 1993. Modulation of gelsolin function: activation at low pH overrides Ca^{2+} requirement. *J. Biol. Chem.* 268:8999–9004.

Lincoln, B., P. L. San Bagio, D. Bulone, J. Newman, C. Hurwitz, H. J. Kinosian, J. E. Estes, and L. C. Gershman. 1998. Actin filaments are structurally weakened by binding of the N-terminal (S1–3) portion of gelsolin. *Biophys J.* 74:A48.

McGough, A., W. Chiu, and M. Way. 1998. Determination of the gelsolin binding site on F-actin: implications for severing and capping. *Biophys. J.* 74:764–772.

McLaughlin, P. J., J. T. Gooch, H. G. Mannherz, and A. G. Weeds. 1993. Structure of gelsolin segment 1-actin complex and the mechanism of filament severing. *Nature.* 364:685–692.

Perrin, D. D., and I. G. Sayce. 1967. Computer calculation of equilibrium concentrations in mixtures of metal ions and complexing species. *Talanta.* 14:833–842.

Pope, B. J., J. T. Gooch, and A. G. Weeds. 1997. Probing the effects of calcium on gelsolin. *Biochemistry*. 36:15848–15855.

Vandekerckhove, J., G. Hauw, K. Vancompernolle, B. Honore, and J. Celis. 1990. Comparative two-dimensional gel analysis and microsequencing identifies gelsolin as one of the most prominent downregulated markers of transformed human fibroblast and epithelial cells. *J. Cell Biol.* 111:95–102.

Vasconcellos, C. A., and S. E. Lind. 1993. Coordinated inhibition of actin-induced platelet aggregation by plasma gelsolin and vitamin D-binding protein. *Blood*. 82:3648–3657.

Way, M., J. Gooch, B. Pope, and A. G. Weeds. 1989. Expression of human plasma gelsolin in *Escherichia coli* and dissection of actin binding sites by segmental deletion mutagenesis. *J. Cell Biol.* 109:593–605.

Weeds, A. G., J. Gooch, P. McLaughlin, B. Pope, M. Bengtsdotter, R. Karlsson. 1995. Identification of the trapped calcium in the gelsolin segment 1-actin complex: implications for the role of calcium in the control of gelsolin activity. *FEBS Lett.* 360:227–230.

Yin, H., and T. P. Stossel. 1979. Control of cytoplasmic actin gel-sol transformation by gelsolin, a calcium-dependent regulatory protein. *Nature.* 281:583–586.

Yin, H., J. H. Hartwig, K. Maruyama, and T. P. Stossel. 1981. Ca^{2+} control of actin filament length by gelsolin: effects of macrophage gelsolin on actin polymerization. *J. Biol. Chem*. 256:9693–9697.

Yu, F-X, D. Zhou, and H. L. Yin. 1991. Chimeric and truncated gCap39 elucidate the requirements for actin filament severing and end capping by the gelsolin family of proteins. *J. Biol. Chem.* 267: 14616–14621.